catalysts

MDPI

Communication

Reduction of Nitrobenzene to Aniline by CO/H_2O in the Presence of Palladium Nanoparticles

Agnieszka Krogul-Sobczak *, Jakub Cedrowski, Patrycja Kasperska and Grzegorz Litwinienko

Faculty of Chemistry, University of Warsaw, Pasteura 1, 02-093 Warsaw, Poland; jcedrowski@chem.uw.edu.pl (J.C.); pkasperska@student.uw.edu.pl (P.K.); litwin@chem.uw.edu.pl (G.L.)

* Correspondence: akrogul@chem.uw.edu.pl

Received: 18 March 2019; Accepted: 24 April 2019; Published: 30 April 2019

Abstract: The transformation of aromatic nitrocompounds into amines by CO/H_2O is catalyzed by palladium(II) complexes. Recently, we have proposed that the catalytic cycle includes Pd^0 as the transient intermediate and herein, for the first time, we describe the application of palladium nanoparticles (PdNPs) stabilized by monodentate N-heterocyclic ligands as nanocatalysts facilitating the reduction of Ar–NO_2 into Ar–NH_2 by CO/H_2O. Among the series—Pd(II) complexes, PdNPs and commercial Pd_{black}—the highest catalytic activity was observed for PdNPs (3.0 ± 0.5 nm) stabilized by 4-Me-pyridine in the presence of 2-Cl-pyridine. The results may be helpful for mechanistic considerations on the role of metallic nanoparticles as active species in other organic processes.

Keywords: aromatic nitrocompounds; aromatic amines; palladium nanoparticles; catalyst; reduction; carbon monoxide; pyridine derivatives

1. Introduction

Aromatic amines are important intermediates and the final products in the chemical and polymer industry [1–5]. Among the commonly applied methods of their synthesis, the reduction of nitroarenes is the most convenient approach. Direct hydrogenation of nitrocompounds undergoes minimal waste generation [6] but is nonselective and expensive [7,8], thus, other methods of reduction are needed for large scale production. One of the most promising methods utilizes the mixture of CO/H_2O as an easily accessible reducing agent [7–11] and is generally described by Equation (1).

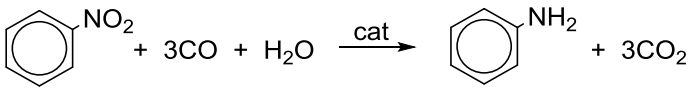

(1)

Recently, we have developed the method of reduction of aromatic nitrocompounds to amines with CO/H_2O, employing $PdCl_2(X_nPy)_2$ complexes as pre-catalysts (X = Cl or CH_3, n = 0 − 2) in the presence of Fe powder and I_2 as co-catalyst and we proposed a plausible mechanism of this process [11,12]. Initially, the traces of aniline are generated from water or ethanol and nitrobenzene (no-catalyst is needed, thus, this step is not included in the main cyclic mechanism presented in Scheme 1) and the formed aniline reacts with the Pd(II) complex [11–14]:

$$PdCl_2(X_nPy_2)_2 + 2PhNH_2 \rightarrow PdCl_2(PhNH_2)_2 + 2X_nPy \quad (2)$$

The subsequent reaction with CO gives N,N′-diphenylurea and trace amounts of Pd^0 (Equation (3)):

$$PdCl_2(PhNH_2)_2 + (z + 1)CO + mX_nPy \rightarrow (PhNH)_2CO + Pd^0(X_nPy)_m(CO)_z + 2HCl \quad (3)$$

where m and z depend on the coordinating ability of Pd(0), amount of X_nPy, and pressure of CO. Pd_{black} is oxidized to Pd^{2+}:

$$Fe^{2+} + 5CO + Pd_{(black)} \rightarrow Fe(CO)_5 + Pd^{2+} \quad (4)$$

by Fe^{2+} cations generated from Fe (powder) and I_2 i.e. co-catalysts [15]. One of the proofs of the Pd^0 presence in the system is the partial precipitation of Pd_{black} [16]. Complex $Pd^0(X_nPy)_m(CO)_z$ formed in reaction (3) reacts with nitrobenzene and carbon monoxide and, at this moment, the catalytic cycle starts; see Scheme 1.

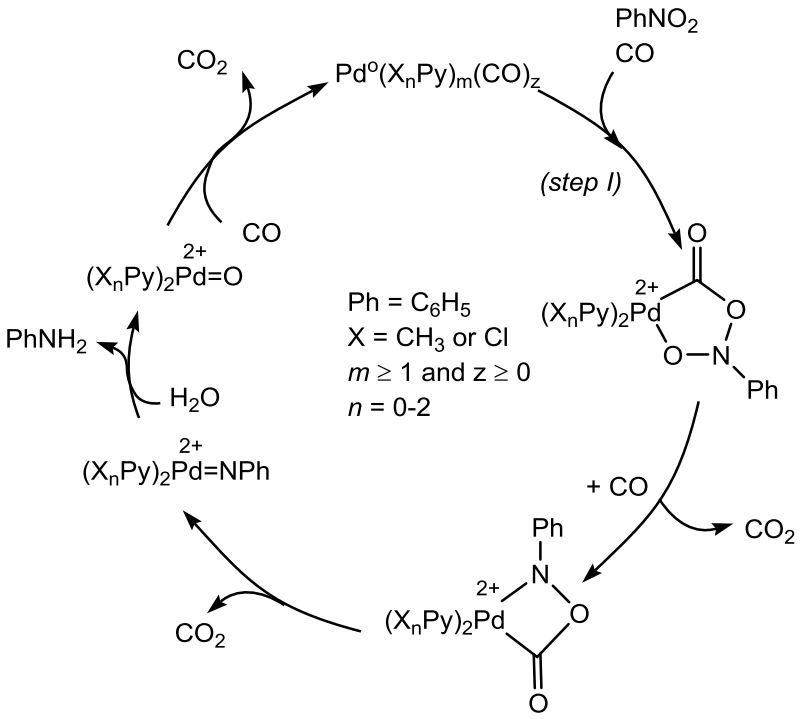

Scheme 1. The proposed mechanism of the reduction of nitrobenzene by CO/H_2O in the presence of Pd^0 formed from $PdCl_2(X_nPy)_2$ complexes [11]. $Pd^0(X_nPy)_m(CO)_z$ is a hypothetical species (with one atom of Pd^0 or it might also be a Pd^0 nanoparticle or cluster stabilized by a non-stoichiometric number of X_nPy ligands and/or CO) that is converted (step I) into a complex of Pd^{2+} as the central ion.

Because nitroaromatic compounds having electron deficient Y substituents ($Y\text{-}C_6H_4NO_2$) undergo a faster reaction, we postulated that the electron transfer from Pd^0 to $Y\text{-}C_6H_4NO_2$ is the rate determining step (RDS). If it is true, the more basic X_nPy ligands (derivatives of pyridine) in $PdCl_2(X_nPy)_2$ should accelerate the catalytic cycle in Scheme 1. Surprisingly, the overall conversion and yield increased with the decreasing basicity of X_nPy, i.e., complexes of chloropyridines were better than methylpyridines [11]. We suppose that increasing the basicity of X_nPy is beneficial for the stability of Pd^0 during RDS described by Equation (5) (see also step I in Scheme 1) but, on the other hand, the very basic pyridine ligand competes with $Y\text{-}C_6H_4NO_2$ for access to the catalytic centre. In this work, we are testing the hypothesis that Pd^0 is involved in the RDS and we are trying to explain the role of X_nPy in RDS.

$$Pd^0(X_nPy)_m + CO + YC_6H_4NO_2 \leftrightarrows [Pd^{2+}(X_nPy)_2(YC_6H_4NO_2)(CO)] + (m-2)X_nPy \quad (5)$$

Formation of Pd^0 in situ as heterogeneous catalysts is in agreement with the mechanisms postulated for other reactions (mainly, hydrogenations) mediated by transition-metal complexes [17] and the common features of such a kind of catalysis are (i) application of easily reduced pre-catalysts, (ii) forcing reaction conditions, and (iii) the presence of nanocluster stabilizers (here: Pd complexes, 180 °C,

4MPa, and N-donor ligands, respectively). In order to verify this hypothesis, we directly applied Pd nanoparticles (PdNPs). The introduction of Pd^0 to the reaction system would increase the rate, as the step of nucleation and formation of Pd^0 (Reactions (2) and (3)) is omitted, and it can give a proof that PdNPs are essential for the catalytic process described by Scheme 1.

During our earlier studies on the catalytic activity of PdNPs/4MePy, we employed a model process of reduction of nitrobenzene to aniline by $NaBH_4$ [18]. We noticed that the size and surface area of nanoparticles (dependent on the way of nanoparticles, NPs, preparation) had a significant impact on their activity and NPs previously dried (before catalytic tests) have higher activity than freshly prepared wet NPs that are transferred directly (after preparation) to the reaction vessel [18]. In this work the catalytic activity of PdNPs is tested for an industrially important process, i.e., the reduction of nitrobenzene (NB) to aniline (AN) by CO/H_2O. To the best our knowledge, there are only a few publications on the reduction of nitro compounds by CO/H_2O performed in the presence of nanoparticles: $Fe(OH)_x$ supported Au nanoclusters [7], hydrotalcite-supported metal nanoparticles [19], TiO_2-supported Au nanoparticles [20] and Co_3O_4/nitrogen doped graphene [21]. Two of the above catalytic systems are based on gold as Au-based catalysts have attracted considerable attention in the past, however, the high effectiveness of palladium (II) complexes in the mentioned process encouraged us to investigate the catalytic activity of PdNPs, which should be potentially more active in comparing the Pd (II) complexes. Compared to bulk catalysts, nanoparticles often possess many unique or improved (catalytic) properties due to the large surface to volume ratio [22] but it is a matter of vivid debate whether the intermediate species generated in situ act as homogeneous and heterogeneous catalysts [17,23–30]. Our goal is to connect the form (size and morphology of PdNPs) and oxidation state of palladium with its catalytic activity in the reduction of NB to AN by CO/H_2O. There is no information in the literature on the application of palladium nanoparticles in the investigated process, therefore, our work provides new knowledge on the catalytic activity of PdNPs. We also study the role of the pyridine ligand during the catalytic process.

2. Results and Discussion

A choice of the stabilizing ligand for PdNPs is extremely important [27,31] because nanocatalysts should effectively interact with both the ligands and with the reacting compound(s). Simple and not bulky derivatives of pyridine (exhibiting a balance between lability and stabilizing properties) seem to be promising candidates for stabilization of NPs [18,32] and this is the first report on the application of PdNPs stabilized by monodentate N-heterocyclic ligands for the reduction of NB to AN by CO/H_2O. Basing on the knowledge that Pd(II) complexes with Cl_yPy ligands (where Y = 1 or 2) exhibited higher catalytic activity than the ones with Me_yPy ligands during the reduction of nitrocompounds using CO/H_2O [11], we tried to generate palladium nanoparticles stabilized by 2ClPy (PdNPs/2ClPy). Unfortunately, we did not succeed with this ligand as a stabilizing agent [18], probably due to its low nucleophilicity [12]. This observation does not refute the hypothesis that Pd^0 is the active species also in the system catalyzed with $PdCl_2(2ClPy)_2$ because in such a case, Pd^0 generated in situ may be instantaneously stabilized by traces of aniline. Taking into account the inability of Cl_yPy to stabilize the PdNPs generated separately, in this work we used other pyridine ligands (Py-ligands): 4-methylpyridine (4MePy), N,N-dimethylaminopyridine (DMAP) and 4-ethylpyridine (4EtPy) as the ligands giving stable NPs [18].

Centrifugation and drying is a common post-synthesis treatment of nanoparticles stabilized by strong (covalently bound) ligands [22,33] and, in this work, we checked how those two methods alter the stability, size and morphology of PdNPs stabilized by Py-ligand. Freshly prepared PdNPs were centrifuged from the raw solution and (a) directly re-suspended in 0.7 mL of ultrapure (Milli-Q, 18.2 MΩ·cm resistivity at 25 °C) water or (b) dried in a vacuum oven (30 °C) and then re-suspended in 0.7 mL of Milli-Q water. TG analysis (see Supplementary Material) shows that Py-ligand is partially desorbed from the surface of PdNPs during the drying process and it might cause the agglomeration of PdNPs. TEM images of PdNPs stabilized by 4MePy (Figure 1), DMAP (Figures S1 and S2) or

4EtPy (Figures S3 and S4) indicate that centrifugation does not significantly influence the size and morphology of PdNPs, whereas the formation of agglomerates is observed for nanoparticles subjected to the drying process.

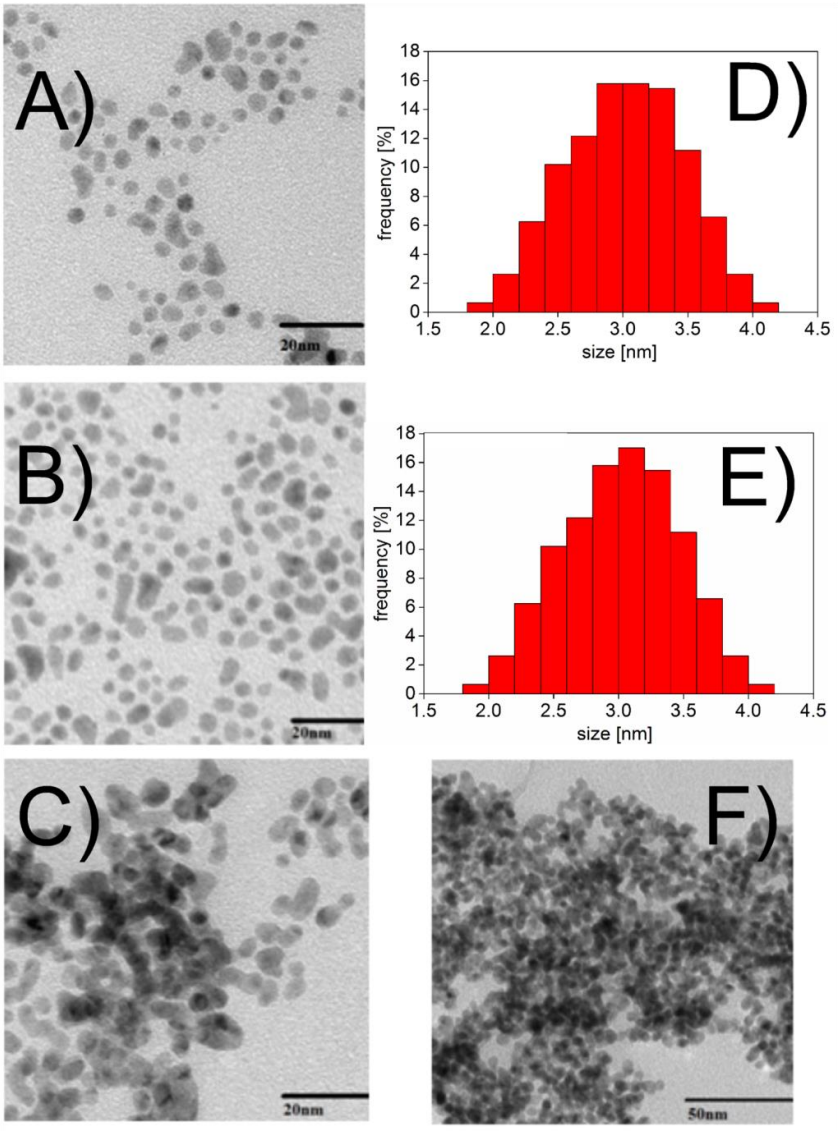

Figure 1. The TEM images of the PdNPs stabilized by 4-methylpyridine (PdNPs/4MePy): raw nanoparticles (NPs) (**A**), centrifuged and suspended (**B**), dried and re-suspended (**C** and **F**: both images present the same NPs but with different magnification). Histograms (evaluated from more than 300 NPs) of size distribution for raw (**D**), and centrifuged (**E**) PdNPs/4MePy. Due to the formation of agglomerates, the histogram was not obtained for "dried" PdNPs. See the Experimental Section for the synthesis conditions. TEM images and particle size distribution determined for PdNPs stabilized by N,N-dimethylaminopyridine and 4-ethylpyridine are provided in Figures S1–S4 in Supplementary Material.

We made efforts to resolve the nature of the active form of Pd catalyst, following the definition given by Schwartz [17,34] for homogeneous catalyst (a metal-complex homogeneous catalyst—monometallic catalyst), and heterogeneous catalyst (nanoclusters, or another metal-particle heterogeneous catalyst—bulk metal). A variety of experiments were proposed to distinguish those two forms of catalysis [17,25,26,35–39] but none of them allows for definitely distinguishing homogeneous catalysis from highly dispersed metal-particle heterogeneous catalysis [17]. Bringing the above discussion into our field, if the mechanism proposed in Scheme 1 is valid, the reduction of NB by

CO/H_2O should be catalyzed not only by Pd (II) complexes (as homogeneous pre-catalyst) but also by PdNPs (as heterogeneous pre-catalysts) stabilized with Py-ligands (4MePy, DMAP, 4EtPy). Catalytic tests were performed according to the general procedure described elsewhere [11]. This system requires water as a reactant (molar ratio of water to nitrobenzene = 1:1) but an excess of water added to the NB/ethanol mixture leads to the formation/separation of the second liquid phase. In order to keep the optimal amount of water in the reacting system, the nanoparticles (0.056 mmol of PdNPs i.e. 0.14%mol vs NB) were previously isolated, purified and re-suspended in 0.7 mL of water and added to the autoclave. The results listed in Table 1 and presented in Figure 2 clearly show that agglomerated NPs were less active catalysts that non-agglomerated (see turnover frequency, TOF, values, entries 4–6,9,10,13,14 for agglomerated and entries 1–3,7,8,11,12 for non-aglomerated NPs). Next, a series of experiments were carried out in order to determine the role of pyridine derivatives in the reaction kinetics. PdNPs stabilized with pyridine ligands were used alone (see entries 1,4,7,9,11,13 in Table 1) or used in the presence of excess 4MePy or 2ClPy (6.2 mmol per 0.056mmol of PdNPs, see footnote *a* in Table 1). The latter derivative was applied because our previous studies showed that $PdCl_2(2ClPy)_2$ complex was a more active catalyst than $PdCl_2(4MePy)_2$ although 2ClPy is a very poor stabilizing ligand for PdNPs (fast precipitation occurs when other ligands are not present). In this work, when PdNPs stabilized by 4MePy, DMAP, or 4EtPy are used as pre-catalyst, the addition of 2ClPy causes a 7 and 11% increase the yield of aniline (entries 2 and 5, respectively). The opposite effect, i.e., a strong decrease of the yield, is observed when the excess of 4MePy is added (see entries 3 and 6 in Table 1).

Table 1. The yield of aniline (Y_{AN}) obtained from the nitrobenzene reduction with CO/H_2O in the presence of 0.056 mmol Pd-species and values of TOF. [a,b]

Entry	Pd-species/Ligand	Additive (XPy)	Y_{AN} [%]	TOF [c]
1	PdNPs [d]/4MePy	-	73	521
2	PdNPs/4MePy	2ClPy	80	571
3	PdNPs/4MePy	4MePy	35	250
4	Pd_{Agglom} [e]/4MePy	-	27	193
5	Pd_{Agglom}/4MePy	2ClPy	38	271
6	Pd_{Agglom}/4MePy	4MePy	10	71
7	PdNPs/DMAP	-	40	286
8	PdNPs/DMAP	2ClPy	48	343
9	Pd_{Agglom}/DMAP	-	20	143
10	Pd_{Agglom}/DMAP	2ClPy	29	207
11	PdNPs/4EtPy	-	54	386
12	PdNPs/4EtPy	2ClPy	62	443
13	Pd_{Agglom}/4EtPy	-	24	171
14	Pd_{Agglom}/4EtPy	2ClPy	37	264
15	Pd_{black}/4MePy [f]	-	12	86
16	Pd_{black}/4MePy [f]	2ClPy	25	179
17	Pd_{black}/4MePy [f]	4MePy	10	71
18 [g]	-	2ClPy	-	0
19	$PdCl_2(4MePy)_2$	-	45	321
20	$PdCl_2(4MePy)_2$	2ClPy	50	357
21	$PdCl_2(4MePy)_2$	4MePy	34	243

[a] Reaction conditions: Pd-species/Fe/I_2 = 0.056/2.68/0.12 mmol; 6.2 mmol XPy (2ClPy or 4MePy); 40 mmol NB; 20 mL ethanol; 0,7 mL water; 180 °C, 40 MPa CO, 60 min. 4MePy = 4-methylpyridine; 4EtPy = 4-ethylpyridine; DMAP = N,N-dimethylaminopyridine; 2ClPy = chloropyridine; AN = aniline; NB=nitrobenzene. [b] Selectivity = 100% (aniline is the only product). [c] TOF_{AN} (turnover frequency for AN) = (mmol of AN formed)(mmol of Pd-species used)$^{-1}h^{-1}$, where mmol of PdNPs corresponds to mmol of Pd in PdNPs/Py-ligand and the composition of Pd/Py-ligand was determined by thermogravimetry (TG) under nitrogen atmosphere with heating rate = 10 K/min, see Figures S5 and S6 in Supplementary Material. [d] PdNPs with average size 3 nm (see Figure 1B) prepared by the method "*a*". [e] Agglomerated PdNPs (see Figure 1C prepared by the method "*b*". [f] 4MePy equal to the percentage of 4MePy in PdNPs/4MePy. [g] Control experiment showed that the reduction of nitrobenzene does not occur in the absence of Pd-based pre-catalyst.

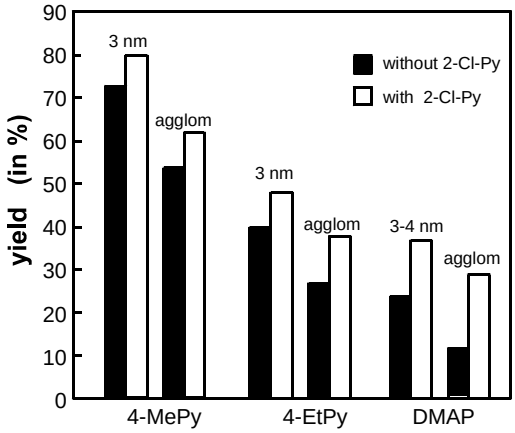

Figure 2. The yield of aniline obtained from nitrobenzene reduction with CO/H_2O in the presence of 0.056 mmol PdNPs stabilized by 4MePy, 4EtPy or DMAP.

Although the positive effect of an excess of 2ClPy (entries 2,5 in Table 1) and the negative effect of an excess of 4MePy (entries 3,6 in Table 1) seems to be counterintuitive, it can be rationalized by the much stronger binding of PdNPs by 4MePy than by 2ClPy ligand. The addition of 100-fold stoichiometric excess of 4MePy over PdNPs makes them perfectly stable, but access to the surface of NPs is strongly restricted. On the other hand, the addition of 2ClPy into the system containing PdNPs stabilized with a small amount of 4MePy results in an equilibrium between chloropyridine and methylpyridine at the metal surface, and some fraction of 2ClPy, as more labile, can be easily replaced by the reacting molecule (see Equation (5)). This interplay of a stronger (in our work 4MePy) and weaker (2ClPy) ligand can be compared to the test described by Finke, with CS_2 being a good binding agent that covers the surface of nanocatalyst and decreases its catalytic activity (however, the CS_2 test is recommended for low temperatures and cannot be used above 50 °C) [39]. Certainly, the presence of both ligands, strong (MePy) and weak (2ClPy), is desirable because the lability of 2ClPy can facilitate the access of substrate to the active surface of the metal. The role of pyridine derivatives is also explained by differences in the catalytic activity of PdNPs stabilized by various pyridine ligands (4MePy, DMAP or 4EtPy). Such results (different yields) cannot be explained by different sizes of PdNPs because, regardless of the stabilizing agent, the size of PdNPs is between 3–4 nm. Perhaps the lowest catalytic activity of PdNPs/DMAP is related to the too-strong electrostatic interactions of NPs with the DMAP ligand.

We also compared the effectiveness of PdNPs/4MePy with other two pre-catalysts: $PdCl_2(4MePy)_2$ complex and the commercially available Pd_{black} and centrifuged PdNPs/4MePy (with a calculated surface of 161 $m^2/g_{(PdNPs)}$, see Supplementary Material) still exhibited the highest activity (entries 1, 15 and 19 in Table 1 and Figure 3). The yields of AN obtained for the two other forms of Pd^0: agglomerated (dried) PdNPs (because of agglomeration a histogram of size distribution was not obtained, thus, the surface was not calculated) and Pd_{black} (with a surface = 40–60 m^2/g, as specified by the producer) are lower compared to the $PdCl_2(4MePy)_2$ complex (entries 1, 4, 15 and 19 in Table 1). The results also indicate that the presence of 2ClPy increases the yield of aniline for those two heterogeneous nanocatalysts, similarly to the system with PdNPs.

If PdNPs are the real active species, the main benefit from the application of PdNPs should be the acceleration of the reaction because nucleation is omitted. However, the yields are comparable to the yields obtained in the presence of $PdCl_2(3,5Cl_2Py)_2$ and $PdCl_2(2ClPy)_2$ [11], and such results indicate that Pd nanoparticles probably act as reservoirs for the formation of homogeneous complexes $Pd^0(X_nPy)_m(CO)_z$ triggering the mechanism presented in Scheme 1.

Although the main scope of our work was to investigate the efficiency of Pd^0 in the catalytic cycle, we also tried to test whether PdNPs can be re-used. The experiments showed that PdNPs/4MePy isolated after a reaction (entry 1 Table 1) by centrifugation and washed with EtOH can be reused in the

next process (the same 73% yield was obtained). However, after the second recovery of PdNPs/4MePy, the yield of the process decreased to half of the starting value. Probably, using supported PdNPs would have been more effective and easier for recovery.

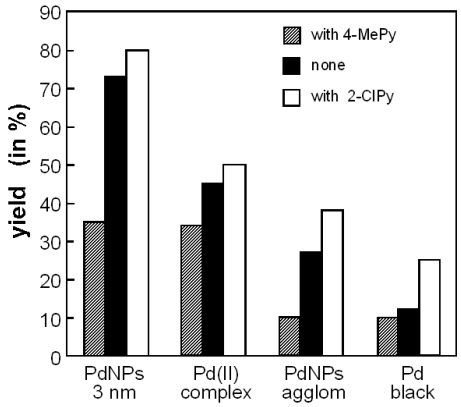

Figure 3. The yield of aniline obtained from nitrobenzene reduction with CO/H_2O in the presence of 0.056 mmol PdNPs/4MePy (3 nm), $PdCl_2(4MePy)_2$ complex, PdNPs (agglomerated) and Pd_{black}/4MePy.

3. Materials and Methods

3.1. Materials

$NaBH_4$, $PdCl_2$, NaCl were used as received. Liquid compounds: pyridine (Py) and substituted pyridines, nitrobenzene (NB), and ethanol, were distilled over the drying agent and stored under argon.

3.2. Synthesis of Palladium Nanoparticles

PdNPs were prepared by the procedure described elsewhere [18]. Briefly, a freshly prepared solution of ligand (a derivative of pyridine; 0.628 mmol in 9 mL of ultrapure water) was added to a stirred solution of NaCl (0.188 mmol; 0.11g) and $PdCl_2$ (0.084 mmol; 0.015 g) in 6 mL of ultrapure water at room temperature. After 20 min of continuous stirring, the mixture was reduced by $NaBH_4$ (1% *w*/*v*, 1.1 mL) and added in 20 µL portions. The progress of the reaction was visually monitored as the mixture progressively changed colour from light orange to dark brown (almost black). The resulting PdNPs were stirred for 30 min.

3.3. Analysis of PdNPs

The size of NPs was measured by Transmission Electron Microscopy (TEM), the observations were carried out using a JEM 1400 microscope (JEOL Co. Tokyo, Japan) at a 120 kV acceleration voltage. The samples were obtained by casting aqueous solution of palladium nanoparticles (0.6 mg/ml^{-1}) onto a carbon coated nickel microgrid (200 mesh) and air-dried overnight.

The composition of Pd/ligand expressed as a percentage of the organic ligand and the metal in palladium nanoparticles stabilized by pyridine ligands was determined by thermogravimetry (TG). The measurements of PdNPs/4-MePy were performed by means of a termogravimeter Q50—1261 TA Instruments (New Castle, DE, USA)—under a nitrogen flow of 6 dm^3/h, with a heating rate = 10 K/min in platinum cells and the weight of the sample was about 8 mg. Weight loss during thermal decomposition of PdNPs/4-MePy was determined in the temperature range 40–600 °C (see Figures S5 and S6 in Supplementary Material). The results presented in this paper is the arithmetic mean of 3 repetitions and the difference of results in a series of determinations of the sample is up to 2%.

X-ray photoelectron spectroscopic (XPS) measurements were performed using a PHI 5000 VersaProbe (ULVAC-PHI, Chigasaki, Japan) spectrometer with monochromatic Al K_α radiation ($h\nu$ = 1486.6 eV). The X-ray beam with a power of 25 W was focused to a diameter of 100 µm with the measured area defined as 250 × 250 µm. The survey spectra were taken in the energy range of 1350–0 eV at the energy

step size of 0.4 eV and the pass energy of 117.4 eV. The high-resolution (HR) XPS spectra were collected with the hemispherical analyzer at the pass energy of 23.5 eV, the energy step size of 0.1 eV and the photoelectron take-off angle 45° with respect to the surface plane. The CasaXPS software (v.2.3.19, Casa Software Ltd, Teignmouth, UK) was used to evaluate the XPS data. All survey spectra were analyzed using the MULTIPAK v.9 software (Chanhassen, MN, USA). The spectra were calibrated against 284.6 eV for the C 1s region. High-resolution spectra of the Pd 3d region were collected for (i) nanoparticles from raw solution, (ii) NPs centrifuged and suspended in ultrapure water, (iii) NPs dried and re-suspended (see Figure S7 in Supplementary Material). For all samples, it was found that the Pd 3d spectrum is an effect of two pairs of spin−orbit components. The Pd $3d_{5/2}$ and $3d_{3/2}$ peaks found at binding energies (BE) = ~335.1 and ~340.3 eV, respectively, are attributed to the metallic Pd^0 [40], while the second pair of Pd 3d signals, at higher BE values (~337.6 and ~342.8 eV), have been associated with Pd^{2+} [40]. Comparison of the peak areas of Pd^0 and Pd^{2+} (after deconvolution, see Figure S7), indicates that 85% of Pd atoms are in the form of Pd^0. However, the XPS results are limited to the surface of NPs and the real content of Pd^0 in the whole sample might be higher than 85%.

Calculation of the surface of PdNPs. Assuming the spherical shape of PdNPs, the surface per gram of Pd [m^2/g] was calculated as a ratio of surface to mass calculated for single PdNPs, see Supplementary Material.

3.4. The Procedure of the Reduction of Nitrobenzene

The reaction was carried out in a 200 mL stainless-steel autoclave equipped with a magnetic stirrer. Pd-based catalyst (0.056 mmol) and Fe powder (2.68 mmol) were subsequently placed in the autoclave, the air was evacuated and the system was filled with purified argon. Then, other reagents and solvents were added under an argon stream: I_2 (0.12 mmol), XPy (6.2 mmol), nitrobenzene (40 mmol), 0.7 mL of water or an aqueous solution of PdNPs, 20 mL of ethanol. The cover was closed and the autoclave was directly filled with carbon monoxide to reach a pressure of 4 MPa, fixed, placed in a hot oil bath and kept at 180 °C for 60 minutes. After the reaction was completed, the autoclave was cooled in the water bath, then vented, and a liquid sample of the reaction mixture was analysed. The yield of the reaction was calculated on the basis of the gas chromatography with Flame Ionization Detector (GC-FID) using n-decyl alcohol as the standard.

4. Conclusions

Comparison of the experiments with PdNPs (stabilized by pyridine ligands) with experiments with Pd(II) complexes (comprising the same pyridine ligands as stabilizing agent for PdNPs), applied respectively as pre-catalysts, showed that Pd^0 is a real active species responsible for the observed catalytic effect, thus, confirming the mechanism proposed in Scheme 1. A significantly higher yield observed for PdNPs compared to Pd_{black} indicates that the catalytically active species are not heterogeneous bulk metal. We suggest that Pd nanoparticles stabilized by pyridine ligands are the most similar to catalytically active reaction intermediates (in agreement with several works indicating the importance of metal-particle heterogeneous catalysis [17,25,27,28]) or that Pd nanoparticles act as reservoirs for the formation of homogeneous complexes (with Pd^0) which are the real catalysts. Based on the obtained results, we postulate that the role of pyridine ligands (with electron-donating substituents) is to stabilize PdNPs whereas the most probable role of ClPy, as the labile ligand, is to facilitate access of the nitro compound to the active surface of the metal. The PdNPs (i) can be obtained with minimal synthetic effort, (ii) exhibit higher catalytic activity than Pd(II) complexes with the same ligand (which is used as a stabilizing agent) or than $Pd_{(black)}$ and, therefore, they have great potential to be applied as a pre-catalyst facilitating reduction by CO/H_2O.

The presented results may be also helpful for mechanistic considerations on the role of metallic nanoparticles in other organic processes based on the application of Pd(II) complexes as pre-catalysts.

Supplementary Materials: The following are available online at http://www.mdpi.com/2073-4344/9/5/404/s1, Figure S1. TEM images of raw PdNPs/DMAP and histogram of particle size distribution; Figure S2. TEM images of

centrifuged PdNPs/DMAP and histogram of particle size distribution; Figure S3. TEM images of raw PdNPs/4EtPy and histogram of particle size distribution; Figure S4. TEM images of centrifuged PdNPs/4EtPy and histogram of particle size distribution; Figure S5. TG curves for centrifuged PdNPs stabilized by 4MePy, DMAP, and 4EtPy; Figure S6. TG curves for centrifuged and dried PdNPs stabilized by 4MePy, DMAP, and 4EtPy; Figure S7. XPS Pd 3d spectra of: A) nanoparticles from raw solution, B) NPs centrifuged and suspended in ultrapure water, C) NPs dried and re-suspended in ultrapure water.

Author Contributions: Investigation, A.K.-S., P.K., and J.C.; conceptualization, conceiving, and planning the experiments, A.K.-S. and G.L.; characterization analysis, A.K.-S.; supervision, original draft preparation, G.L. and A.K.-S. All authors discussed the results and contributed to the final manuscript.

Funding: This work was funded by the National Science Centre-Poland, grant OPUS decision no. 2014/15/B/ST4/04835. Publication costs were partially covered by University of Warsaw.

Acknowledgments: The authors acknowledge the support from the National Science Centre-Poland, grant OPUS decision no. 2014/15/B/ST4/04835. We also thank Wiktor Lewandowski for helpful discussion on the XPS spectra.

Conflicts of Interest: The authors declare no conflict of interest. The funders had no role in the design of the study; in the collection, analyses, or interpretation of data; in the writing of the manuscript, or in the decision to publish the results.

References

1. Ono, N. *The Nitro Group in Organic Synthesis*; Wiley: Hoboken, NJ, USA, 2003.
2. Tafesh, A.M.; Weiguny, J. A Review of the Selective Catalytic Reduction of Aromatic Nitro Compounds into Aromatic Amines, Isocyanates, Carbamates, and Ureas Using CO. *Chem. Rev.* **1996**, *96*, 2035–2052. [CrossRef] [PubMed]
3. Ragaini, F. Away from phosgene: Reductive carbonylation of nitroarenes and oxidative carbonylation of amines, understanding the mechanism to improve performance. *Dalton Transactions* **2009**, *32*, 6251–6266. [CrossRef]
4. Downing, R.S.; Kunkeler, P.J.; vanBekkum, H. Catalytic syntheses of aromatic amines. *Catal. Today* **1997**, *37*, 121–136. [CrossRef]
5. Vogt, P.F.; Gerulis, J.J. Amines, Aromatic. In *Ullmann's Encyclopedia of Industrial Chemistry*; Gerhartz, W., Ed.; Wiley-VCH Verlag GmbH & Co. KGaA: New York, NY, USA, 2000; Available online: https://onlinelibrary.wiley.com/doi/abs/10.1002/14356007.a02_037 (accessed on 18 March 2019).
6. Zhao, S.L.; Liang, H.D.; Zhou, Y.F. Selective hydrogenation of m-dinitrobenzene to m-nitroaniline. catalyzed by PVP-Ru/Al2O3. *Catal. Commun.* **2007**, *8*, 1305–1309. [CrossRef]
7. Liu, L.Q.; Qiao, B.T.; Chen, Z.J.; Zhang, J.; Deng, Y.Q. Novel chemoselective hydrogenation of aromatic nitro compounds over ferric hydroxide supported nanocluster gold in the presence of CO and H_2O. *Chem. Commun.* **2009**, *6*, 653–655. [CrossRef] [PubMed]
8. Ambrosi, A.; Denmark, S.E. Harnessing the Power of the Water-Gas Shift Reaction for Organic Synthesis. *Angew. Chem. Int. Ed.* **2016**, *55*, 12164–12189. [CrossRef]
9. Cann, K.; Cole, T.; Slegeir, W.; Pettit, R. Catalytic Reductions Using Carbon-Monoxide and Water in Place of Hydrogen. 2. Reduction of Aromatic Nitro-Compounds to Amines. *J. Am. Chem. Soc.* **1978**, *100*, 3969–3971. [CrossRef]
10. Nomura, K. Efficient Selective Reduction of Aromatic Nitro-Compounds by Ruthenium Catalysis under Co/H_2O Conditions. *J. Mol. Catal. A: Chem.* **1995**, *95*, 203–210. [CrossRef]
11. Krogul, A.; Litwinienko, G. Application of Pd(II) Complexes with Pyridines as Catalysts for the Reduction of Aromatic Nitro Compounds by CO/H_2O. *Org. Process Res. Dev.* **2015**, *19*, 2017–2021.
12. Krogul, A.; Skupinska, J.; Litwinienko, G. Catalytic activity of $PdCl_2$ complexes with pyridines in nitrobenzene carbonylation. *J. Mol. Catal. A: Chem.* **2011**, *337*, 9–16. [CrossRef]
13. Giannoccaro, P. Reactivity of Mono-Methoxycarbonyl and Di-Methoxycarbonyl Complexes of Pd(II) Towards Amines and Copper Amine Complexes - Role of Copper in the Catalyzed Palladium Copper Oxidative Carbonylation of Amines. *J. Organomet. Chem.* **1994**, *470*, 249–252. [CrossRef]
14. Skupinska, J.; Karpinska, M. Nitrobenzene transformations in the carbonylation reaction in the presence of the $PdCl_2$/Fe/I_2/Py catalyst system. *Appl. Catal. A-Gen.* **2004**, *267*, 59–66. [CrossRef]

15. Skupinska, J.; Karpinska, M.; Olowek, M.; Kasprzycka-Guttman, T. The effect of the components of the $PdCl_2$/Fe/I_2/Py catalytic system on nitrobenzene carbonylation to ethyl N-phenylcarbamate. *Cen. Eur. J. Chem.* **2005**, *3*, 28–39. [CrossRef]
16. Ragaini, F.; Cenini, S. Mechanistic studies of palladium-catalysed carbonylation reactions of nitro compounds to isocyanates, carbamates and ureas. *J. Mol. Catal. Chem.* **1996**, *109*, 1–25. [CrossRef]
17. Widegren, J.A.; Finke, R.G. A review of the problem of distinguishing true homogeneous catalysis from soluble or other metal-particle heterogeneous catalysis under reducing conditions. *J. Mol. Catal. A Chem.* **2003**, *198*, 317–341. [CrossRef]
18. Krogul-Sobczak, A.; Kasperska, P.; Litwinienko, G. N-heterocyclic monodentate ligands as stabilizing agents for catalytically active Pd-nanoparticles. *Catal. Commun.* **2018**, *104*, 86–90. [CrossRef]
19. Mikami, Y.; Noujima, A.; Mitsudome, T.; Mizugaki, T.; Jitsukawa, K.; Kaneda, K. Highly Chemoselective Reduction of Nitroaromatic Compounds Using a Hydrotalcite-supported Silver-nanoparticle Catalyst under a CO Atmosphere. *Chem. Lett.* **2010**, *39*, 223–225. [CrossRef]
20. He, L.; Wang, L.-C.; Sun, H.; Ni, J.; Cao, Y.; He, H.-Y.; Fan, K.-N. Efficient and Selective Room-Temperature Gold-Catalyzed Reduction of Nitro Compounds with CO and H2O as the Hydrogen Source. *Angew. Chem. Int. Ed.* **2009**, *48*, 9538–9541. [CrossRef]
21. Westerhaus, F.A.; Sorribes, I.; Wienhofer, G.; Junge, K.; Beller, M. Reduction of Nitroarenes Using CO and H_2O in the Presence of a Nanostructured Cobalt Oxide/Nitrogen-Doped Graphene (NGr) Catalyst. *Synlett* **2015**, *26*, 313–317. [CrossRef]
22. Feng, J.; Handa, S.; Gallou, F.; Lipshutz, B.H. Safe and Selective Nitro Group Reductions Catalyzed by Sustainable and Recyclable Fe/ppm Pd Nanoparticles in Water at Room Temperature. *Angew. Chem. Int. Ed.* **2016**, *55*, 8979–8983. [CrossRef]
23. Astruc, D.; Lu, F.; Aranzaes, J.R. Nanoparticles as recyclable catalysts: The frontier between homogeneous and heterogeneous catalysis. *Angew. Chem. Int. Ed.* **2005**, *44*, 7852–7872. [CrossRef] [PubMed]
24. Astruc, D. Palladium nanoparticles as efficient green homogeneous and heterogeneous carbon-carbon coupling precatalysts: A unifying view. *Inorg. Chem.* **2007**, *46*, 1884–1894. [CrossRef]
25. Phan, N.T.S.; Van Der Sluys, M.; Jones, C.W. On the nature of the active species in palladium catalyzed Mizoroki-Heck and Suzuki-Miyaura couplings—Homogeneous or heterogeneous catalysis, a critical review. *Angew. Chem. Int. Ed.* **2006**, *348*, 609–679.
26. Pun, D.; Diao, T.N.; Stahl, S.S. Aerobic Dehydrogenation of Cyclohexanone to Phenol Catalyzed by Pd(TFA)(2)/2-Dimethylaminopyridine: Evidence for the Role of Pd Nanoparticles. *J. Am. Chem. Soc.* **2013**, *135*, 8213–8221. [CrossRef]
27. Wang, D.; Weinstein, A.B.; White, P.B.; Stahl, S.S. Ligand-Promoted Palladium-Catalyzed Aerobic Oxidation Reactions. *Chem. Rev.* **2018**, *118*, 2636–2679. [CrossRef]
28. Crabtree, R.H. Resolving Heterogeneity Problems and Impurity Artifacts in Operationally Homogeneous Transition Metal Catalysts. *Chem. Rev.* **2012**, *112*, 1536–1554. [CrossRef] [PubMed]
29. Lewis, L.N. Chemical catalysis by colloids and clusters. *Chem. Rev.* **1993**, *93*, 2693–2730. [CrossRef]
30. Aiken, J.D.; Finke, R.G. A review of modern transition-metal nanoclusters: Their synthesis, characterization, and applications in catalysis. *J. Mol. Catal. A: Chem.* **1999**, *145*, 1–44. [CrossRef]
31. Amiens, C.; Ciuculescu-Pradines, D.; Philippot, K. Controlled metal nanostructures: Fertile ground for coordination chemists. *Coord. Chem. Rev.* **2016**, *308*, 409–432. [CrossRef]
32. Flanagan, K.A.; Sullivan, J.A.; Mueller-Bunz, H. Preparation and characterization of 4-dimethylaminopyridine-stabilized palladium nanoparticles. *Langmuir* **2007**, *23*, 12508–12520. [CrossRef]
33. Megiel, E. Surface modification using TEMPO and its derivatives. *Adv. Colloid Interface Sci.* **2017**, *250*, 158–184. [CrossRef]
34. Schwartz, J. Alkane activation by oxide-bound organorhodium complexes. *Acc. Chem. Res.* **1985**, *18*, 302–308. [CrossRef]
35. Whitesides, G.M.; Hackett, M.; Brainard, R.L.; Lavalleye, J.P.P.M.; Sowinski, A.F.; Izumi, A.N.; Moore, S.S.; Brown, D.W.; Staudt, E.M. Suppression of Unwanted Heterogeneous Platinum(0)-Catalyzed Reactions by Poisoning with Mercury(0) in Systems Involving Competing Homogeneous Reactions of Soluble Organoplatinum Compounds - Thermal-Decomposition of Bis(Triethylphosphine)-3,3,4,4-Tetramethylplatinacyclopentanet. *Organometallics* **1985**, *4*, 1819–1830.

36. Crabtree, R.H.; Mellea, M.F.; Mihelcic, J.M.; Quirk, J.M. Alkane Dehydrogenation by Iridium Complexes. *J. Am. Chem. Soc.* **1982**, *104*, 107–113. [CrossRef]
37. Lewis, L.N. On the Mechanism of Metal Colloid Catalyzed Hydrosilylation - Proposed Explanations for Electronic Effects and Oxygen Cocatalysis. *J. Am. Chem. Soc.* **1990**, *112*, 5998–6004. [CrossRef]
38. Hornstein, B.J.; Aiken, J.D.; Finke, R.G. Nanoclusters in catalysis: A comparison of CS2 catalyst poisoning of polyoxoanion- and tetrabutylammonium-stabilized 40 +/- 6 angstrom Rh(0) nanoclusters to 5% Rh/Al2O3, including an analysis of the literature related to the CS2 to metal stoichiometry issue. *Inorg. Chem.* **2002**, *41*, 1625–1638. [PubMed]
39. Widegren, J.A.; Bennett, M.A.; Finke, R.G. Is it homogeneous or heterogeneous catalysis? Identification of bulk ruthenium metal as the true catalyst in benzene hydrogenations starting with the monometallic precursor, Ru(II)(eta(6)-C6Me6)(OAC)(2), plus kinetic characterization of the heterogeneous nucleation, then autocatalytic surface-growth mechanism of metal film formation. *J. Am. Chem. Soc.* **2003**, *125*, 10301–10310.
40. Liu, C.-H.; Liu, R.-H.; Sun, Q.-J.; Chang, J.-B.; Gao, X.; Liu, Y.; Lee, S.-T.; Kang, Z.-H.; Wang, S.-D. Controlled synthesis and synergistic effects of graphene-supported PdAu bimetallic nanoparticles with tunable catalytic properties. *Nanoscale* **2015**, *7*, 6356–6362. [CrossRef]